Relativistic Effects in Electron Scattering from Atoms*

A. C. YATES† AND T. G. STRAND‡
Department of Chemistry, Indiana University, Bloomington, Indiana
(Received 13 December 1967)

Relativistic and nonrelativistic differential cross sections for argon, krypton, and iodine are computed for the energy range 20 eV–150 keV. The atomic fields as determined by Clementi (Hartree-Fock) and Liberman (Dirac) are used interchangeably in the two calculations. Contributions to the cross section arising from exchange between incident and atomic electrons are also considered. Relativistic and nonrelativistic comparisons are made, and where available, the experimental data are also reproduced. A number of conclusions regarding relativistic and exchange effects are reached, most noteworthy of which are the low-energy exchange effects.

I. INTRODUCTION

A SERIES of recent papers[1–4] has been concerned with the question of the importance of relativistic effects at low energies, but as yet no serious theoretical attempt has been made to obtain accurate quantitative results. The aim of the present paper, then, is to investigate these effects in the energy range 30 eV–150 keV. Although no new numerical techniques have been introduced, care has been taken in selecting the most efficient methods of solving both the relativistic and nonrelativistic problems.

In the following sections we discuss the atomic potentials used, together with an analytic representation of electron exchange between atomic and incident electrons. The methods of calculation are given in some detail in Sec. III, while Sec. IV contains the results of our calculations and points out the more significant features of the calculated curves.

II. DESCRIPTION OF THE CALCULATION

A. Potential

Cox and Bonham[5] have obtained potential field parameters by the least-squares fitting of analytic expressions to radial electron density curves $D(r)$. In several cases two sets of parameters for a sum of Yukawa terms are given for the same atom, corresponding to fits of $D(r)$ curves calculated by either Liberman[6] or Clementi.[7] The Clementi curves were obtained using Hartree-Fock wave functions, whereas Liberman's results are from solutions of the Dirac equation using Hartree-Fock-Slater wave functions. The screened atomic potential can be written in Yukawa form as[8,9]

$$V_s(r)=\frac{Z}{r}\sum_i \gamma_i e^{-\lambda_i r}, \tag{2.1}$$

where the γ_i's and λ_i's are the potential field parameters described above. With the potential as represented analytically by (2.1), the electron charge density $\rho(r)$ can be written as

$$\rho(r)=\frac{Z}{4\pi r}\sum_i \gamma_i\lambda_i^2 e^{-\lambda_i r}. \tag{2.2}$$

It is well known[10] that effects arising from the exchange between the atomic and scattered electrons become increasingly more important with decreasing incident electron energies. Liberman[11] has suggested that the exchange approximation proposed by Gaspar[12] be incorporated into the total potential representing the electron scattering problem, which may be written as

$$V_x=(1/\pi)[3\pi^2\rho(r)]^{1/3}. \tag{2.3}$$

Thus in the present approximation[13] the total potential is written as

$$V_t=V_s+V_x. \tag{2.4}$$

The potential field parameters for $Z=18$, 36, 53, and 54 are reproduced in Table I.

B. Calculation of Phase Shifts

The central problem in the calculation of elastic cross sections is the determination of phase shifts, the exact values of which must be obtained from numerical solution of the radial Dirac and Schrödinger equations.

* Publication No. 1548 from the Chemical Laboratories of Indiana University. The authors wish to thank the U. S. Air Force Office of Scientific Research for its support of this work.
† NDEA Predoctoral Fellow in Chemical Physics.
‡ Present address: Department of Chemistry, University of Oslo, Blindern, Norway.
[1] H. N. Browne and E. Bauer, Phys. Rev. Letters **16**, 495 (1966).
[2] M. Rotenberg, Phys. Rev. Letters **16**, 969 (1966).
[3] L. Spruch, Phys. Rev. Letters **16**, 1137 (1966).
[4] John F. Dawson, Phys. Rev. **163**, 71 (1967).
[5] H. L. Cox, Jr., and R. A. Bonham, J. Chem. Phys. **47**, 2599 (1967).
[6] D. Liberman, J. T. Waber, and Don T. Cromer, Phys. Rev. **137**, A27 (1964).
[7] E. Clementi, J. Chem. Phys. **38**, 996 (1963); **38**, 1001 (1963).
[8] All equations are written in Hartree atomic units; e.g., the unit of length is $a_0=0.529168$ Å.
[9] See, e.g., R. A. Bonham and T. G. Strand, J. Chem. Phys. **39**, 2200 (1963).
[10] N. F. Mott and H. S. W. Massy, *The Theory of Atomic Collision* (Oxford University Press, London, 1965), Chap. XVIII.
[11] D. Liberman (private communication).
[12] R. Gaspar, Acta Phys. Hung. **3**, 263 (1954).
[13] We do not include effects arising from polarization of the atomic electron cloud caused by the incident electron, but we do expect that such effects are most important in the small-angle region (see Ref. 10).

TABLE I. Potential field parameters γ_i and λ_i.

$Z=18$				$Z=36$				$Z=53$		$Z=54$	
γ_i [a]	λ_i [a]	γ_i [b]	λ_i [b]	γ_i [a]	λ_i [a]	γ_i [b]	λ_i [b]	γ_i [b]	λ_i [b]	γ_i [b]	λ_i [b]
1.4268[c]	2.1236[d]	1.0494	1.9051	4.6222	7.2780	4.1201	7.2511	7.5470	13.0998	7.6397	13.6666
−0.0602	46.3176	−0.0512	18.2836	−0.0484	85.3334	−0.0553	85.3351	−0.9267	137.7790	−0.0299	137.4095
4.6440	5.7689	4.5976	6.1771	12.8497	13.1155	11.8935	12.8260	20.9226	23.1825	21.5995	24.0007
7.4701	16.7556	7.5956	16.3783	14.6739	33.2254	13.7167	36.0695	20.1441	47.7586	20.8424	48.7608
−4.4056	4.5419	−3.8659	5.0032	−1.6424	2.8197	−1.3169	2.6894	−5.0227	7.5548	−5.1302	7.8087
−8.0771	15.8867	−8.3311	15.4957	−15.3978	11.3682	−14.3716	11.2830	−24.3363	20.4409	−25.0317	21.1625
				−15.5805	32.3498	−14.2991	35.2590	−21.9987	46.5394	−22.8271	47.4972
				1.5224	2.0998	1.3121	1.9907	1.4709	8.8768	1.5368	9.1558
								2.1230	4.7276	2.1983	4.9962
								0.1963	0.8271	0.2210	0.8904

[a] Clementi parameters. [b] Liberman parameters. [c] Dimensionless. [d] Hartree atomic units.

The nonrelativistic phase shifts η_l are determined from the solutions of the radial Schrödinger equation,

$$d^2u_l(r)/dr^2+[k^2+2V(r)-l(l+1)/r^2]u_l(r)=0. \quad (2.5)$$

Solution of this equation and subsequent calculations of phase shifts can be efficiently effected using the "phase-amplitude method" described in detail by Peacher and Wills.[14] We add only that the integration scheme described by Peacher was compared with the more elegant Adams-Moulton predictor-corrector routine[15] as a check for accuracy and stability.

The two-component Dirac equation for the scattering problem can be written[16] as

$$\alpha_+F_l(r)+dG_l(r)/dr+[(1+n)/r]G_l(r)=0, \quad (2.6)$$
$$\alpha_-G_l(r)+dF_l(r)/dr+[(1-n)/r]F_l(r)=0.$$

By eliminating the small component F_l and making the substitution

$$G_l(r)=\alpha_+^{1/2}g_l(r)/r,$$

Eq. (2.6) can be written in the Schrödinger form

$$d^2g_l(r)/dr^2+[k^2-l(l+1)/r^2-U_l(r)]g_l(r)=0, \quad (2.7)$$

where the Dirac potential U_l is

$$-U_l(r)=2\gamma V(r)+\alpha^2V^2(r) - \frac{n}{r}\frac{\alpha_+'}{\alpha_+}-\frac{3}{4}\left(\frac{\alpha_+'}{\alpha_+}\right)^2+\frac{1}{2}\frac{\alpha_+''}{\alpha_+}. \quad (2.8)$$

Also we have

$$n=-(l+1), \quad j=l+\tfrac{1}{2} \quad (2.9)$$
$$= \quad l, \quad j=l-\tfrac{1}{2}$$

and

$$\alpha_\pm=(\gamma\pm1)/\alpha+\alpha V(r), \quad (2.10)$$

where l is the orbital angular momentum quantum number, j is the total angular momentum quantum number, and n takes on two values corresponding to the two spin states. The symbol α is the usual Sommerfeld fine-structure constant and γ is the relativistic correction factor $\gamma=(1-v^2/c^2)^{-1/2}$. A relativistic wave vector was used in both the relativistic and nonrelativistic calculations, the magnitude of which is given by $k^2=\alpha^{-2}(\gamma^2-1)$. Asymptotically the solution of (2.7) in the region where $V(r)\simeq0$ can be written as[17]

$$g_l(r)=j_l(kr)\cos\delta_l-n_l(kr)\sin\delta_l,$$

where j_l and n_l are the spherical Bessel functions of the first and second kind, respectively; δ_l is the Dirac phase shift. At this point the convenient change of variables[18,19]

$$F_l(r)=A_l(r)[\sin\varphi_l(r)]/r, \quad (2.11)$$
$$G_l(r)=A_l(r)[\cos\varphi_l(r)]/r \quad (2.12)$$

was employed, which leads to

$$d\varphi_l/dr=(n/r)\sin2\varphi_l +\gamma/\alpha+\alpha V(r)-(1/\alpha)\cos2\varphi_l. \quad (2.13)$$

With little effort one finds that the phase shifts can be determined from

$$\tan\delta_l=\frac{kj_{l+1}(kr)-j_l(kr)\{(1/\alpha)(\gamma+1)[\tan\varphi_l(r)](1+l+n)/r\}}{kn_{l+1}(kr)-n_l(kr)\{(1/\alpha)(\gamma+1)[\tan\varphi_l(r)](1+l+n)/r\}}, \quad (2.14)$$

[14] J. L. Peacher and J. G. Wills, J. Chem. Phys. 46, 4809 (1967).
[15] We wish to thank G. Eckley for use of his predictor-corrector routine.
[16] See Ref. 10, Chap. IV.
[17] L. I. Schiff, *Quantum Mechanics* (McGraw-Hill Book Co., New York, 1955), p. 104.
[18] S. Lin, N. Sherman, and J. R. Percus, Nucl. Phys. 45, 492 (1963).
[19] P. J. Bunyan and J. L. Schonfelder, Proc. Phys. Soc. (London) 85, 455 (1965).

TABLE II. Exact phase shifts (in radians) for argon at 20 eV and 40 keV.

	20 eV				40 keV		
l	η_l	$\eta_{l\text{-exch}}$	δ_l	δ_{-l-1}	η_l	δ_l	δ_{-l-1}
0	7.1294	8.0882	7.1486		1.2869	1.2885	
1	4.5764	5.7365	4.5803	4.5946	0.9472	0.9458	0.9717
2	0.5052	2.3704	0.5052	0.5056	0.7771	0.7755	0.7877
5	0.0022	0.1869	0.0021	0.0021	0.5240	0.5228	0.5272
10		0.0142			0.3376	0.3368	0.3387
15		0.0012			0.2419	0.2414	0.2424
20					0.1841	0.1837	0.1844
25					0.1454	0.1451	0.1455
30					0.1172	0.1170	0.1174
35					0.0956	0.0954	0.0957
40					0.0784	0.0783	0.0785
45					0.0644	0.0643	0.0644
50					0.0529	0.0528	0.0529

where the right side is evaluated at a point where $V(r)\simeq 0$. Hence, we have only to integrate (2.13) out to the matching radius. This can be done quite efficiently using a fifth-order Kutta algorithm[20] (the Euler-Romberg procedure[21] was used as a check for stability).

The solution is started by expanding $\varphi_l(r)$ and $V(r)$ in a power series in r, e.g.,

$$V(r)=\frac{Z}{r}\sum_{i=0} c_i r^i, \tag{2.15}$$

where the c_i's are determined from (2.1); also

$$\varphi_l(r)=\sum_{i=0} a_i r^i. \tag{2.16}$$

The expansion coefficients a_i may be determined successively by substituting (2.15) and (2.16) into (2.13). Using these expansions the phase shifts were found to be insensitive to changes in the starting values of $r\leq 0.001$.

WKB and Born phase shifts were also calculated where applicable. The phase shifts as derived from the WKB solutions of Good[22] are, with $\rho=kr$,

$$\delta_l=\int_{\rho_0}^{\infty}\left\{\left[A(\rho)-(l+1)(l+\tfrac{1}{2})\right]\rho^{-1}+\frac{l+1}{2k}\frac{\alpha_+'}{\alpha_+}\right\}\times[A(\rho)-(l+1)^2]^{-1/2}d\rho-\int_{|l+1|}^{\infty}[\rho^2-(l+1)(l+\tfrac{1}{2})]\times[\rho^2-(l+1)^2]^{-1/2}\rho^{-1}d\rho, \tag{2.17}$$

where ρ_0 is the zero of the denominator and

$$A(\rho)=\rho^2\{[1+2\gamma+\alpha V(\rho)]V(\rho)/k^2\}. \tag{2.18}$$

The nonrelativistic phase shift η_l is obtained by setting the third term in (2.18) and the term containing α_+ in (2.17) equal to zero. If the denominators of the integrals in (2.17) are factored and the change of variable $\rho=l^2+\rho_0$ is made, then the integrals may be routinely evaluated using Gauss-Legendre quadrature formulas. The roots were obtained by Newton-Raphson iteration.

The Born phase-shift formula[23] using (2.1) reduces to

$$\eta_l=\frac{2Z\gamma}{k}\sum_i \gamma_i Q_l(1+\lambda_i^2/2k^2), \tag{2.19}$$

where Q_l is the Legendre function of the second kind. The Dirac phase shifts δ_l and δ_{-l-1} can be written approximately in terms of the Born nonrelativistic phases η_l as[24]

$$\delta_l=-\frac{1}{2}\frac{m+m_0}{m}\left(\eta_l+\frac{m-m_0}{m+m_0}\eta_{l+1}\right) \tag{2.20a}$$

and

$$\delta_{-l-1}=-\frac{1}{2}\frac{m+m_0}{m}\left(\eta_l+\frac{m-m_0}{m+m_0}\eta_{l-1}\right), \tag{2.20b}$$

where m is the relativistic electron mass and m_0 is the electron rest mass.

Table II provides a comparison of phase shifts for the relativistic and nonrelativistic cases for $Z=18$ at electron energies of 20 eV and 40 keV.

C. Calculation of Cross Sections

The differential cross sections are defined as

$$d\sigma/d\Omega=|f(\theta)|^2+|g(\theta)|^2, \tag{2.21}$$

with

$$f(\theta)=\frac{1}{2ik}\sum_l\{(l+1)[\exp(2i\delta_l)-1]+l[\exp(2i\delta_{-l-1})-1]\}P_l(\cos\theta), \tag{2.22}$$

$$g(\theta)=\frac{1}{2ik}\sum_l[\exp(2i\delta_{-l-1})-\exp(2i\delta_l)]P_l^1(\cos\theta) \tag{2.23}$$

for the relativistic case, and

$$d\sigma/d\Omega=|f(\theta)|^2, \tag{2.24}$$

where

$$f(\theta)=\frac{1}{2ik}\sum_l(2l+1)[\exp(2i\eta_l)-1]P_l(\cos\theta) \tag{2.25}$$

for the nonrelativistic case. The phase-shift series (2.22), (2.23), and (2.25) were summed by applying the reduced-series method of Yennie, Ravenhall, and

[20] W. E. Milne, *Numerical Solution of Differential Equations* (John Wiley & Sons, Inc., New York, 1955), Chap. V.
[21] T. R. McCalla, *Introduction to Numerical Methods and Fortran Programming* (John Wiley & Sons, Inc., New York, 1967), Chap. IX.
[22] R. H. Good, Jr., Phys. Rev. **90**, 131 (1952).
[23] T. Wu and T. Ohmura, *Quantum Theory of Scattering* (Prentice-Hall, Inc., Englewood Cliffs, N. J., 1962), Chap. I.
[24] G. Parzen, Phys. Rev. **80**, 261 (1950).

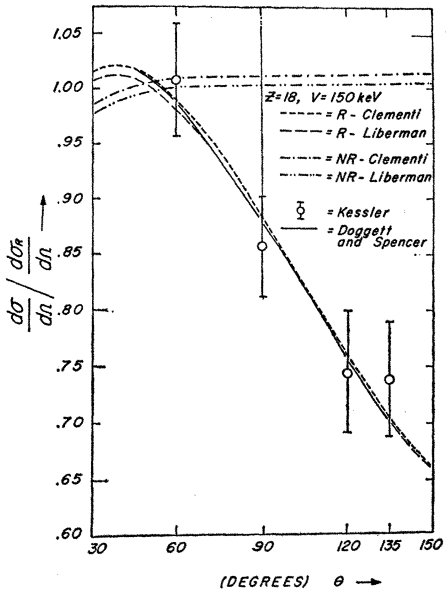

FIG. 1. Calculated relativistic and nonrelativistic elastic cross sections for argon at 150 keV compared to that given by experiment. $d\sigma_R/d\Omega$ is the Rutherford cross section.

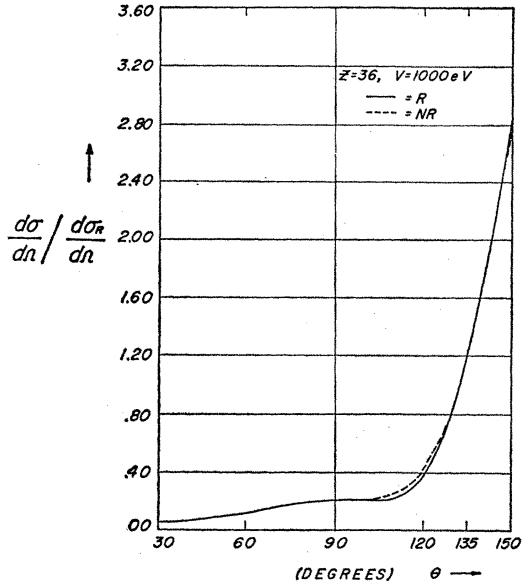

FIG. 2. Relativistic and nonrelativistic elastic cross sections, calculated for krypton at 1000 eV. $d\sigma_R/d\Omega$ is the Rutherford cross section.

Wilson[25] for faster convergence. This method is applicable to any series of Legendre polynomials; e.g., if

$$h(\cos\theta)=\sum_l a_l P_l(\cos\theta),$$

then the recurrence formula for $P_l(\cos\theta)$ effects the transformation

$$(1-\cos\theta)^m h(\cos\theta)=\sum_l a_l{}^m P_l(\cos\theta),$$

where

$$a_l{}^{m+1}=a_l{}^m-\left(\frac{l+1}{2l+3}\right)a_{l+1}{}^m-\left(\frac{l}{2l-1}\right)a_{l-1}{}^m.$$

For our calculations it was found that two reductions on each series were adequate to give the desired accuracy, as determined by comparison with the corresponding direct summations which were carried out until six-figure stability was obtained. All sums were done using double precision arithmetic.[26]

III. RESULTS AND CONCLUSION

The results of our calculations are presented in Figs. 1–4. A comparison with experiment is made where measured values are available. Differential cross sections for argon and krypton were computed for electron energies of 40 and 150 keV. Figure 1 shows the series of curves obtained for argon at 150 keV, together with the experimental points measured by Kessler,[27] and the corresponding theoretical curve of Doggett and Spencer.[28] The curves are plotted as the ratio of our calculated cross sections to the Rutherford cross section $d\sigma_R/d\Omega$ versus scattering angle, where

$$d\sigma_R/d\Omega=(2Z\gamma/a_0 s^2)^2,$$

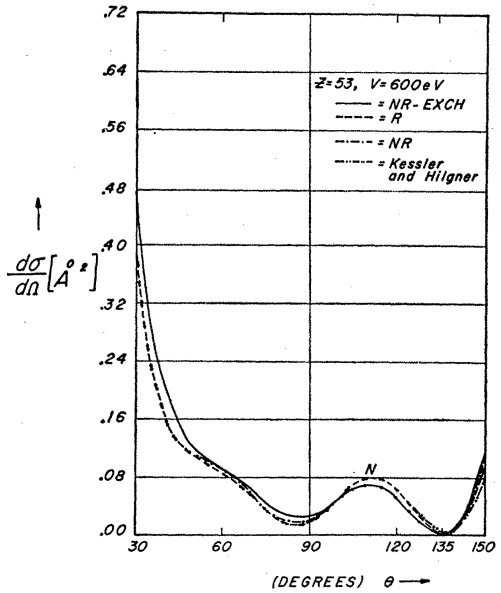

FIG. 3. Elastic cross sections calculated for atomic iodine and compared to experimental data on I_2 at 600 eV. N is the normalization point. Note that the experimental curve follows the relativistic curve closely throughout the entire energy range.

[25] D. R. Yennie, D. G. Ravenhall, and R. N. Wilson, Phys. Rev. 95, 500 (1954).

[26] All calculations were performed on the CDC 3600 computer, wherein 25 significant figures are returned for double precision variables.

[27] J. Kessler, Z. Physik 155, 350 (1959).

[28] J. A. Doggett and L. V. Spencer, Phys. Rev. 103, 1597 (1956).

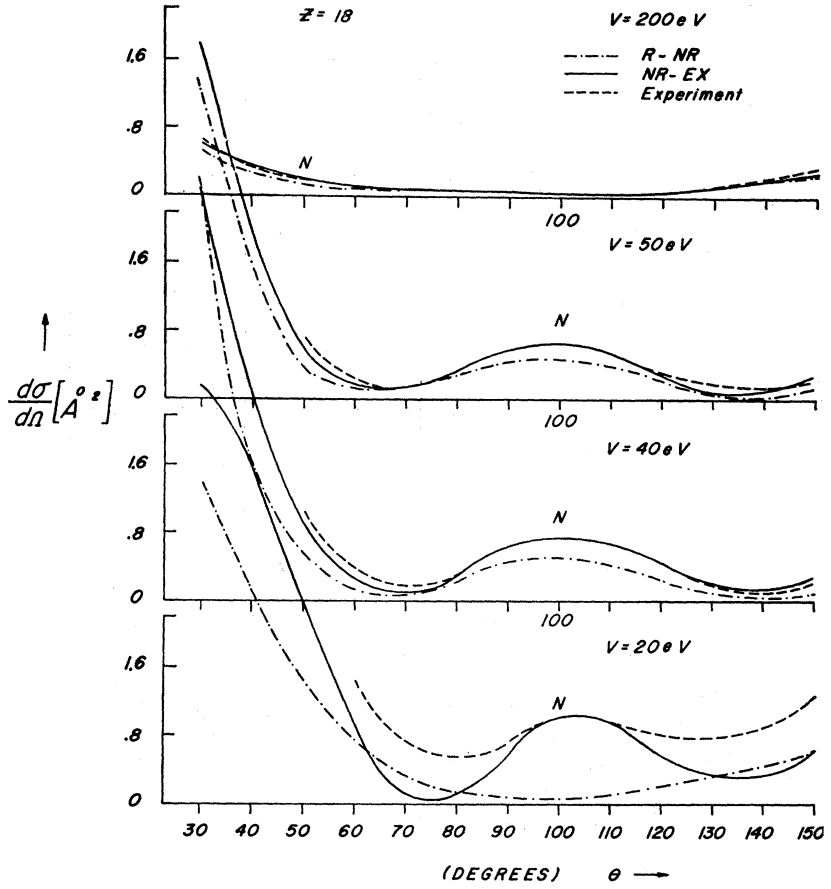

FIG. 4. Low-energy calculations of elastic cross sections for argon at 20, 40, 50, and 200 eV compared with experiment. N is the normalization point.

with $s=2k\sin\frac{1}{2}\theta$, and a_0 is the first Bohr radius. The 40- and 150-keV curves for both argon and krypton show, as expected, that the nonrelativistic treatment does not adequately represent the experiment qualitatively or quantitatively at either energy. In the limit of very high electron energies and large angles the nonrelativistic ratios should approach unity, as predicted by theory; the small deviations shown here are primarily due to the screening and show small effects even at the largest scattering angles. Further evidence of the relative unimportance of screening for argon (i.e., with respect to the cross section) is shown by noting the agreement between our relativistic curves and Doggett and Spencer's Coulomb cross section. However, greater differences are found for krypton (not shown), which implies that the effect of screening increases with increasing atomic number. A further result of the high-energy calculation is that no particular improvement is made if one uses either the Liberman or the Clementi parameters, which would imply that the primary relativistic effects are the result of the description of the scattering process rather than the atomic field.

Figure 2 shows that even for electron energies as high as 1000 eV relativistic effects are no longer very important for krypton (identical results were obtained for argon). However, our calculated curves for iodine (Fig. 3) show, in agreement with Browne and Bauer,[1] that relativistic effects increase with increasing atomic number, but the deviations are not nearly as great as those predicted by these workers. Figure 3 is also interesting for other reasons. The measurements done by Hilgner and Kessler[29] are made for I_2 and the close agreement with our relativistic curve, calculated for the atom, indicates that molecular effects are quite small. A comparison of the atomic cross section to that given by the independent atom model[10] for I_2 shows that the contributions arising from the molecular interference terms are less than 5%.

The series of curves given in Fig. 4 represent a summary of our low-energy calculations. Curves labelled R-NR (relativistic and nonrelativistic) are actually two curves and show explicitly that the two descriptions yield nearly identical cross sections at these energies (analogous results were also found for krypton). As expected the curves show the decreasing applicability of the usual screened Coulomb static potential with decreasing energies. This is supported by the fact that the best fit of the experimental data is provided by the

[29] W. Hilgner and J. Kessler, Phys. Rev. Letters 18, 983 (1967).

curves including exchange. Below about 30 eV, calculations not allowing for exchange (and possible distortion and polarization effects) are seemingly quite meaningless, as can be seen from the 20-eV curves. As the energy increases, the experiment becomes less sensitive to the exchange potential until, finally, relativistic effects predominate. The experimental results are those of Mehr.[30]

In view of the fact that a controversy has erupted[1–4] over the magnitudes of relativistic corrections for low-energy scattering the results reported here have a special relevance. The current state of scattering theory and many-body theory does not allow us to easily decide the issue discussed by these authors on theoretical grounds alone. Fortunately good experimental data on relative differential elastic cross sections are available for a large number of atoms for electron scattering energies as low as 20 to 30 eV. This experimental work coupled with the calculations reported here shows that relativistic effects are small (at least smaller than 5%) and that all the recent data for $\theta=30°$ to 150° at energies from 40 eV up can be explained to within the experimental error of the data by use of relativistic or nonrelativistic partial-wave scattering theory utilizing static, relativistic or nonrelativistic, self-consistent-field wave functions for the atom, coupled with the free-electron exchange potential employing the same atomic field. It is curious to note that no evidence exists in the angular and energy ranges studied for charge polarization effects of the type reported in earlier work.[31] If significant charge polarization exists it must be less dependent on the size of the atom and confined to a much smaller angular range than previously thought.

The present results also point out the sensitivity of the low-energy scattering to the exchange correction. This observation suggests that low-energy results can provide useful information about the nature of atomic and molecular fields.

[30] J. Mehr, Z. Physik **198**, 345 (1967).
[31] See Ref. 10, pp. 577–586.

At the higher energies in the same angular range ($30°<\theta<150°$) relativistic effects become increasingly important. Again the results presented here are in excellent agreement with the available experimental results. The ratio of the relativistic differential cross section to the Rutherford nonrelativistic cross section is quite different from the ratio obtained using the nonrelativistic result in the numerator. Unfortunately the shape of this ratio appears to be relatively insensitive to the choice of the potential field used for the scatterer and appears to be largely a function of the atomic number and the use of the Dirac equation to describe the scattering process. The actual differences in the cross sections using relativistic or nonrelativistic static fields amounted to less than 1% in the worst cases for the angular range that was studied.

In summarizing the results of our calculations on argon, krypton, and iodine we find that relativistic effects

(a) invariably increase with increasing electron energies,

(b) increase slightly with increasing atomic number,

(c) when important under (a) and (b), are relatively insensitive to the atomic field representation in the angular region 30°–150° and from 20 eV to 150 keV (except through the exchange term), and

(d) at energies below about 200 eV are relatively unimportant and are far overshadowed by exchange and possibly other effects.

ACKNOWLEDGMENTS

We are especially grateful to Professor R. A. Bonham for suggesting this problem and also for this continued interest and assistance throughout. We further wish to thank Dr. Manfred Fink for reading the manuscript and for many helpful discussions. Finally, we thank the Indiana University Research Computing Center for use of its facilities.